Equilibration of air temperature inside the thimble of a Farmer-type ion chamber

R. C. Tailor[a)]
Department of Radiation Physics, The University of Texas M. D. Anderson Cancer Center, Houston, Texas 77030

C. Chu
LDS Hospital, Salt Lake City, Utah

D. S. Followill and W. F. Hanson
Department of Radiation Physics, The University of Texas M. D. Anderson Cancer Center, Houston, Texas 77030

(Received 21 July 1997; accepted for publication 14 January 1998)

Ionization chambers are frequently moved from one environment to another, sometimes with significant differences in temperature between the chamber and measurement phantom. To obtain reliable ionization data, the temperature of the air in the chamber must be allowed to equilibrate with the measuring phantom. The air temperature inside a thimble of a Farmer-type ion chamber was measured as a function of time for various phantom materials (air, water, and plastic). Equilibration rates for the various conditions are presented. Heat-diffusion theory is presented to explain the characteristics of the measured data. Waiting times for temperature equilibration down to 10% of the initial temperature difference ranges from 1 to 18 min, depending on the phantom material and use of bare or covered thimble. Radiation measurements confirm the temperature data. [S0094-2405(98)00104-7]

Key words: temperature, ionization chamber, phantom, equilibration, dosimetry

I. INTRODUCTION

The Radiological Physics Center (RPC) currently monitors approximately 1200 institutions participating in inter-institutional cooperative clinical trials funded by the National Cancer Institute (NCI). During its on-site dosimetry review visits to these institutions, the RPC team determines and observes both photon and electron output calibrations in various phantom materials including air, water, and various plastics. The RPC has observed errors in temperature measurements of the phantom material ranging up to 2 °C. These errors result from either (i) an inappropriate point of temperature measurement or (ii) insufficient waiting time for thermal equilibration between the temperature probe and the phantom material. The point of temperature measurement requires a little elaboration. In the case of an in-air output calibration, for example, an appropriate place to measure air temperature is in the vicinity of the beam isocenter. If it is measured elsewhere in the room, however, the air temperature may be appreciably different, depending on the location of air-conditioning or exhaust vents. In the case of an output calibration in a plastic phantom, one may incur significant error by assuming the phantom temperature to be the same as that of the surrounding air, for two reasons. First, a plastic phantom takes several hours to equilibrate with the surrounding air temperature, as reported by Barish[1] and confirmed by our measurements. Second, the temperature of a plastic phantom may be significantly different from the temperature measured by a thermometer on the wall or in the vicinity of the beam isocenter even if the phantom has been sitting in the same room for several hours, but in a remote area or in a cabinet. Phantoms stored in a closet in the treatment room may be significantly warmer than the ''air'' in the room. Even greater temperature differences may exist between the cabinet in a physics laboratory and the air in a treatment room due to different room-temperature settings and positioning of air-conditioning vents.

Kubo[2] provides equilibration data for three cylindrical ion chambers in air and in water, and for a parallel-plate chamber in air and polystyrene. Giessen[3] presents temperature-change data for a nylon-thimble chamber in air, water, and polystyrene. Mayo *et al.*[4] present data supporting the argument that a cylinder chamber with an air-equivalent plastic thimble exhibits a change in thimble dimensions with temperature, an effect not seen for a graphite-thimble chamber. The time constants reported by Kubo vary by a factor of 2 for different chambers in both air and water, and by a factor of 2–4 from that reported by Giessen in water. In air, the two author's data overlap.

This work presents more extensive data, improves precision of the data, indicates the presence of a shoulder and multiple components to the exponential equilibration curves. Thus a single temperature constant is probably not adequate. In addition, our ionization data, as that of Mayo, fail to identify any measurable thermal expansion/contraction of a graphite thimble.

Temperature measurements inside the thimble of a Farmer-type ion chamber have been made as a function of time in air, water, and plastic media. In each case, tempera-

ture difference is plotted versus time on a semi-log scale. Distinct differences in the thermal equilibration between the different types of media are noted and discussed. Negligible differences were seen between conductive or nonconductive thimble material and between heating and cooling rates. The thermal-equilibration curves are verified by heat-diffusion theory. Further, the temperature measurements are confirmed by ionization measurements in a plastic medium.

II. MATERIALS AND METHODS

Direct temperature measurements were made inside the thimble of an 0.6 cc Farmer-type NEL chamber (Nuclear Enterprises, Ltd., Fairfield, NJ) equipped with either a graphite-coated nylon or a graphite thimble. The central electrode was replaced by a thin (0.005-in.-diam) thermocouple (type E) which provides a fast temperature response. The temperature reader was an Omega model 450 AET (Omega Engineering, Inc., Stamford, CT 06907). A similar thermocouple and reader were used to monitor the temperature of the phantom material. Temperature was recorded in °F because that scale provided the higher resolution (0.1 °F). The plastic phantom consisted of a stack of 1 cm and 2 cm thick, 30 cm×30 cm slabs of high-impact polystyrene, model RW-3 (Nuclear Associates, Division of Victoreen, Inc., Carle Place, NY 11514) measuring 14.5 cm of total thickness. A large temperature-controlled water bath (45 cm ×30 cm×30 cm) with continuous stirring was used to establish the initial temperature of the ion chamber or plastic phantom to 10–20 °F below or above the ambient air temperature. For all measurements, a digital clock with hour/minute/second read-out was used. The digital read-out of the clock and thermocouples were simultaneously recorded with a camcorder. Data were captured by playback of the videotape in stop-frame mode.

To study the cooling rate of the plastic phantom, all slabs were separated and kept immersed in the hot water bath ($\approx$100 °F) for $\sim$1 h. Individual slabs were removed from the water, quickly dried with paper towels, and stacked in a Styrofoam box for heat insulation. Thermocouple probes were placed at three locations between the middle slabs of the plastic phantom as indicated in Fig. 1. The entire plastic phantom was assumed to be at an initially uniform temperature inside the Styrofoam box. The phantom was then removed from the Styrofoam box and placed on a wooden table, exposing it to ambient air on five sides. This marked zero time.

The study of the thermal equilibration of an ion chamber in air was accomplished (i) with a bare thimble, and (ii) with the thimble covered with a Co-60 build-up cap (0.46-cm Lucite wall). The chamber with (or without) the build-up cap was placed in a water-proofing rubber sleeve (0.2 mm thick) and immersed in the water bath at a temperature $\sim$10 °F warmer (or cooler) than the surrounding air temperature. When the chamber reached thermal equilibrium ($\geqslant$30 min), it was removed from the water bath, the water-proofing sleeve removed, and the chamber exposed to ambient air. This marked zero time.

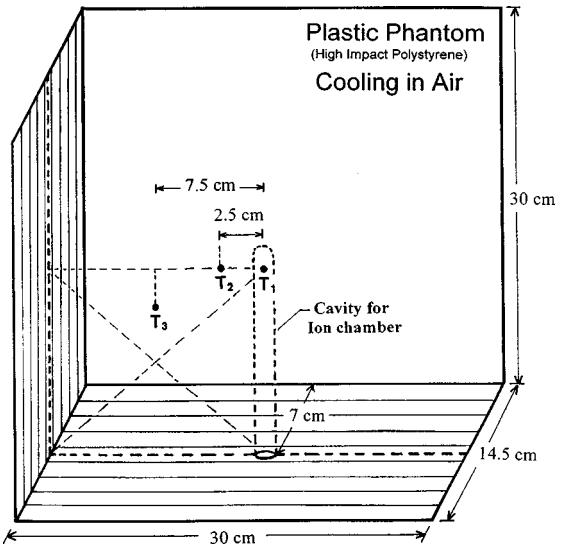

FIG. 1. Cross section of the middle slabs of the plastic phantom. The ion-chamber cavity and position of the thermocouples are indicated.

To study the thermal equilibrium of an ion chamber in water, the water-bath temperature was established to $\sim$10 °F warmer (or cooler) than the surrounding room-air temperature. For the bare-thimble study, the protective cap (0.46 cm Lucite) was maintained in the water phantom to assure thermal equilibration of the cap with the water bath. The chamber was then inserted into the protective cap that marked zero time. Similar data were acquired by inserting the chamber with its build-up cap (at room temperature) into the water phantom at time zero.

To study the thermal equilibration of an ion chamber in a plastic phantom, the phantom was thermally stabilized in the water bath to a temperature $\sim$10–15 °F warmer (or cooler) than the ambient air. The chamber (bare thimble) at room temperature was then inserted into the phantom, marking zero time.

For ionization measurements in the plastic phantom, the radiation source was a Co-60 ''Eldorado 8'' unit (Atomic Energy of Canada Ltd., Kanata, Canada). The phantom was thermally stabilized in the water bath to a temperature $\sim$10–15 °F warmer or cooler than the ambient air. The ion chamber (bare thimble) was thermally stabilized in ambient air. Insertion of the chamber into the phantom marked time zero. Ionization produced inside the thimble was measured in the rate mode with a Keithley model 602 electrometer (Keithley Instruments, Inc., Cleveland, OH), modified by CNMC (CNMC Company, Nashville, TN) to provide a digital read-out. The digital read-out of the electrometer was included in the time/temperature data acquisition by the camcorder.

III. RESULTS AND DISCUSSION

We shall denote the time after zero time as t, the temperature difference between the ''chamber'' and the phantom as ΔT, the initial temperature difference as ΔT_0, and the initial phantom temperature as T_0. All data are presented as semi-log plots of the normalized temperature difference, $\Delta T/\Delta T_0$,

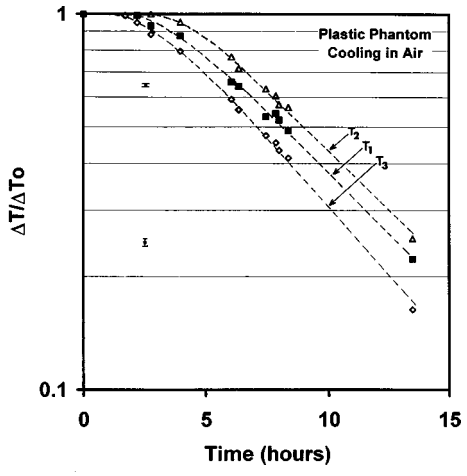

FIG. 2. Cooling plots of a high-impact polystyrene phantom as the phantom cools from near 100 °F to room temperature. Data for the three thermocouples indicated in Fig. 1 are included. Errors bars represent a resolution of 0.1 °F.

versus time, which we will refer to as cooling or warming plots. The normalization facilitates intercomparison of the measured data sets. The error bars in Figs. 2–6 represent an estimate of uncertainty based on the precision of ± 0.1 °F in the temperature measurements. All plots have a common characteristic, i.e., an initial shoulder region (sizable or negligible) followed by a one-, two- or multicomponent exponential fall-off. As the next section, Theoretical Basis, explains, the initial shoulder represents a delay in heat transmission through a barrier separating the point of measurement and the warmer or cooler medium.

Typical cooling plots for the plastic phantom are presented in Fig. 2. The three sets of data indicated by different symbols correspond to temperature measurements at the three sites identified in Fig. 1. The trends of the data are shown as dashed curves. The three curves differ primarily in the width of the shoulder. Since the width of the shoulder represents a time delay in heat transfer through the slab-wall thickness, temperature (T_2) at a deeper position has a broader shoulder as compared to T_3 at the shallower position. The temperature (T_1) inside the cavity, although it is the deepest position, does not show the broadest shoulder due to faster heat transfer through the air in the cavity. The final slopes of the exponential fall-off are not significantly different for the three curves. The three data points near the tails of the trend lines all appear to be below the trend lines, probably due to the drift in the surrounding air temperature, especially over a period of several hours. However, an uncertainity originating from the temperature drift is included

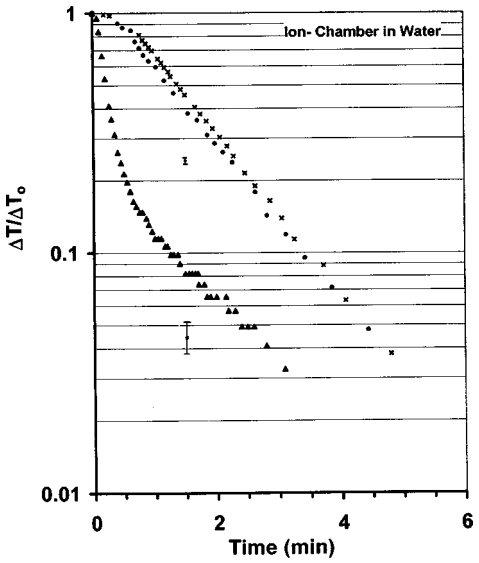

FIG. 4. Cooling/warming curves for an ion chamber in a water phantom. Data are presented for a bare ion chamber cooling (▲) and for a chamber in a Lucite cap (Co-60 build-up) cooling (**x**) and warming (●). Errors bars represent a resolution of 0.1 °F.

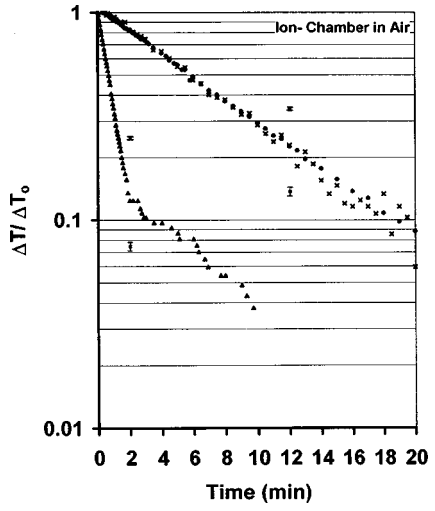

FIG. 3. Cooling/warming curves for an ion chamber in air. Data are presented for the bare thimble with no buildup cap cooling (▲), and for the chamber in its buildup cap warming (●). Also included are cooling data from ionization measurements (**x**). Errors bars represent a resolution of 0.1 °F.

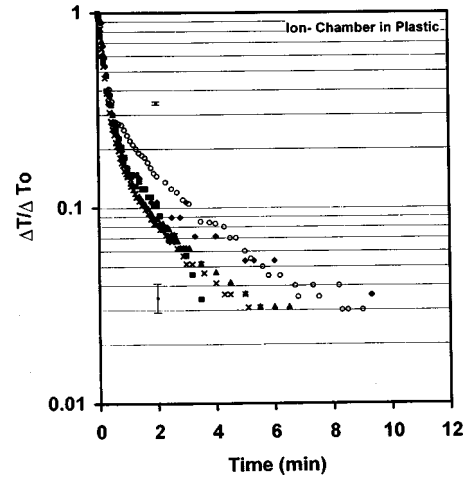

FIG. 5. Cooling/warming curves for an ion chamber in a plastic phantom. Five sets of data (four sets warming and one cooling) were taken over the course of one year. Errors bars represent a resolution of 0.1 °F.

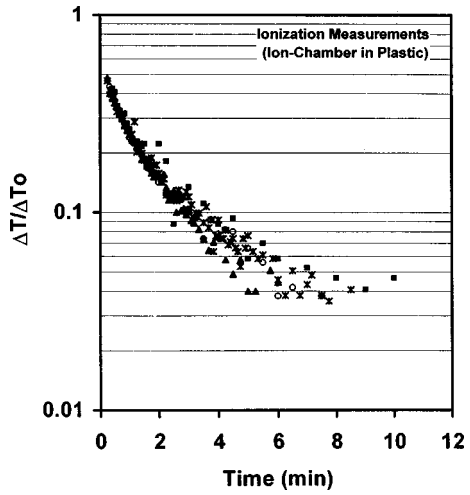

FIG. 6. Cooling/warming curves for an ion chamber in a plastic phantom derived from ionization measurements. Data represent four sets measured over 1 year.

in the error bars shown. The plastic phantom required ~15 h for the temperature difference, ΔT, to diminish to 20% of ΔT_0. The exact equilibration time depends on material, size of the phantom and the location of the point of measurement inside the phantom. R. J. Barish[1] reported that the temperature difference diminished to the 50% level after 1.7 h. Barish's measurements at 1-cm depth below the top surface of a 25 cm×25 cm×5.2 cm clear polystyrene (SCRAD) phantom inside the chamber cavity in contact with the wall simulated measurements near d_{max}. Our measurements, at 7-cm depth to simulate photon-beam calibration at depth, resulted in a much longer equilibration time. Comparison of the measured data with a theoretical solution is presented and discussed in the next section.

The data in Fig. 3 represent thermal equilibration of a Farmer-type ion chamber in air. The solid-circle symbols represent warming of the chamber and build-up cap in air. The initial shoulder (width 0.5 min) represents a delay in heat transmission through the 0.46-cm Lucite wall of the build-up cap. The shoulder is followed by a single-exponential fall-off. Ionization measurements were made in a Co-60 beam with a similar ion chamber and build-up cap cooling in air. The change in ionization readings was then used to deduce the change in temperature of the air inside the thimble using the ideal gas law. The cross symbols in Fig. 3 represent the ionization data converted to temperature-change data. The ionization and the direct temperature measurements are in excellent agreement. The solid-triangle symbols represent cooling of the chamber with a bare thimble in air. The absence of the shoulder in these data indicates a negligible delay in heat transmission through the thimble because of negligible wall thickness (0.036-cm Nylon). As expected, temperature equilibration is much faster because there is no build-up cap. These data show more than a one-component exponential fall-off. The initial fall-off, until ΔT reaches close to 10% of ΔT_0, is a fast component, whereas the latter fall-off is much slower and perhaps arises from continuation of heat transfer from the stem of the chamber. The stem, because of insulating contents and large heat capacity, takes longer to equilibrate with the surrounding air.

The data in Fig. 4 represent thermal equilibration of an ion chamber in a water phantom. The solid circle and cross symbols represent cooling and warming data, respectively, when the chamber along with its build-up cap are inserted into the water phantom. The two sets of data corresponding to warming and cooling are in good agreement within measurement error. The initial shoulder, representing a delay in heat transmission through the 0.46-cm Lucite wall of the build-up cap, is followed by a single-component exponential fall-off similar to that of the chamber with build-up cap in Fig. 3. Equilibration is about a factor of 5 faster in water than in air. The solid-triangle symbols represent the data for insertion of the ion chamber's bare thimble into a build-up cap already at thermal equilibrium in the water phantom. The initial shoulder is absent as exhibited previously by the bare-thimble data in Fig. 3. The second exponential component is again probably attributable to the influence of the stem.

Figure 5 shows data for the ion chamber's thermal equilibration in a plastic phantom. The cross symbols correspond to cooling, while all others correspond to warming. The four data sets representing warming correspond to repeated measurements performed over a 1 year period. All sets show good agreement in the initial fall-off region, but divergence begins after ΔT drops below 30% of ΔT_0. The spread among the repeat sets is attributed to poor reproducibility of the contact between the thimble and the plastic phantom. The characteristics of rapid equilibration, negligible shoulder, and double exponential components are typical of the bare chamber in all media. The initial exponential component is comparable to that in the corresponding case in air.

Figure 6 presents ionization measurements converted to temperature using the ideal gas law for the thermal equilibration of the ion chamber in a plastic phantom. Since the Co-60 unit was preset to treat, the radiation measurements could begin within a few seconds of time zero. The four different symbols correspond to four sets of data (two for cooling and two for warming) of the chamber inside the plastic phantom. The temperature measurements indicated somewhat faster equilibrium than the ionization measurements. Although both sets of data show reasonable scatter with some overlap of the two sets, the difference may represent the time lag between the temperature change and the change in the mass of the gas inside the thimble. If so, this indicates a time lag of some fraction of a minute.

The issue of thimble's volume change causing departure from the ideal gas law was addressed by Mayo *et al.*[4] They concluded, from ionization measurements, that the departure from the ideal gas law was 20% for ''air equivalent'' plastic thimble and negligible for graphite thimble. Our data sets for both graphite and nylon thimbles are in good agreement and indicate negligible deviation from the ideal gas law.

IV. THEORETICAL BASIS

Two of the experimental conditions were modeled theoretically for solutions. The cooling of the plastic phantom was approximated by a semi-infinite slab, and the equilibration of the ion chamber with build-up cap in water was modeled by a semi-infinite cylinder.

Consider a semi-infinite plastic slab of thickness, L, with its two surfaces at $x=0$ and $x=L$. Assume that the slab is initially at a uniform temperature, T_0, and is exposed at time zero to a surrounding medium that would maintain the slab's two surfaces at zero temperature. Subsequently, at time, t, the temperature, T, inside the slab at a position, x, is governed by the thermal-conduction equation:[5,6]

$$\frac{\delta^2 T}{\delta x^2}=\left(\frac{\rho C}{K}\right)\frac{\delta T}{\delta t}, \tag{1}$$

where K is the thermal conductivity, ρ is the density, and C is the specific heat of the plastic. The solution[2] of this equation, at the center of the slab ($x=L/2$), simplifies to

$$T=\frac{4T_0}{\pi}\sum_{n=\text{odd}}\frac{1}{n}\left[\exp\left\{-\frac{n^2\pi^2 Kt}{(L^2\rho C)}\right\}\right]\left[\sin\left(\frac{n\pi}{2}\right)\right]$$

or

$$\frac{T}{T_0}=\frac{4}{\pi}\left[y^t-\frac{1}{3}y^{9t}+\frac{1}{5}y^{25t}-\frac{1}{7}y^{49t}+\cdots\right], \tag{2}$$

where

$$y=\exp[-\pi^2 K/(L^2\rho C)].$$

In general, if a surrounding medium maintains the slab's surfaces at any arbitrary temperature (not necessarily zero), the above solution may be rewritten as

$$\frac{\Delta T}{\Delta T_0}=\frac{4}{\pi}\left[y^t-\frac{1}{3}y^{9t}+\frac{1}{5}y^{25t}-\frac{1}{7}y^{49t}+\cdots\right], \tag{3}$$

where ΔT and ΔT_0 refer to temperature differences with respect to the surrounding air at any time t and time $t=0$, respectively. Since the exponential term, y, is always less than one, the series in the above equation is convergent. In the region, $t\gg[L^2\rho C/(\pi^2 K)]$, the first term dominates and Eq. (3) reduces to

$$\frac{\Delta T}{\Delta T_0}=\frac{4}{\pi}\exp\left[-\frac{\pi^2 Kt}{(L^2\rho C)}\right]. \tag{4}$$

This equation represents an exponential decay of $\Delta T/\Delta T_0$. The factor $[\pi^2 K/(L^2\rho C)]$ may be identified as decay constant, λ, and the equation may be rewritten to represent a straightline for $\ln(\Delta T/\Delta T_0)$ versus t:

$$\ln(\Delta T/\Delta T_0)=-\lambda t+\ln(4/\pi). \tag{5}$$

In the region, $t<[L^2\rho C/(\pi^2 K)]$, the higher-order terms become more significant and Eq. (3) exhibits a shoulder. We may define the shoulder width, $\mathfrak{I}$, quantitatively as the projected time based on linear Eq. (5) for ΔT to be equal to ΔT_0.

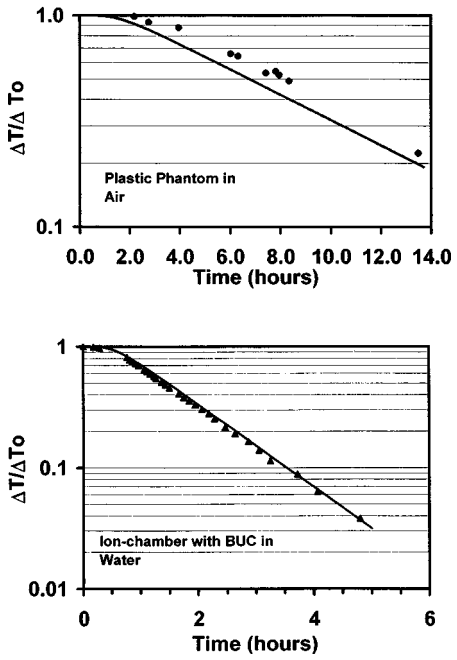

FIG. 7. Comparison of theory and experiment for two cases. The theoretical curves are plotted as solid lines, and the experimental data are marked as data points.

Thus

$$\mathfrak{I}=[\ln(4/\pi)]/\lambda. \tag{6}$$

Consider next, an infinitely long cylinder of radius, R, initially at a known uniform temperature, and a surrounding medium capable of maintaining the cylinder's surface at some other known steady temperature. At time zero, the cylinder is introduced into the medium. At a later time, t, the temperature difference, ΔT, between the cylinder's axis and the medium, obtained after simplification of the solution[6] of the thermal-conduction equation, is given by

$$\frac{\Delta T}{\Delta T_0}=2\sum_{n=1}^{\infty}\left[\exp\left\{-\frac{\beta_n^2 Kt}{(R^2\rho\pi C)}\right\}\right]\Big/[\beta_n J_l(\beta_n)], \tag{7}$$

where ΔT_0, ΔT, K, and C are defined above. The β_n are the positive real values of β for which the zero-order Bessel function, $J_0(\beta)$, becomes zero, and $J_1(\beta_n)$ are the values of the first-order Bessel function for the corresponding β_n values. The series is convergent. In the region, $t\gg[R^2\rho C/(\beta_1^2 K)]$, the first term dominates and Eq. (7) reduces to

$$\Delta T/\Delta T_0=2[\exp\{-\beta_1^2 Kt/(R^2\rho C)\}]/[\beta_1 J_1(\beta_1)]. \tag{8}$$

The decay constant, λ, and the shoulder width, $\mathfrak{I}$, as defined earlier, are given by

$$\lambda=\beta_1^2 K/(R^2\rho C) \tag{9}$$

and

$$\mathfrak{I}=\{\ln(2/[\beta_1 J_1(\beta_1)])\}/\lambda. \tag{10}$$

TABLE I. Results of thermal equilibration of ion chamber introduced into various phantom media.

Phantom medium	Thimble covering[a]	Initial-shoulder width (minutes)	Number of exponential components in fall-off region	Half-life of the first exponential component (minutes)	Time length (minutes) to reach a specific % of ΔT_0		
					50%	10%	Comment
Air	Co-60 build-up cap[b]	0.5	1	5.2	5.7	18	longest
	bare thimble	None	2	0.7	0.7	3.0	···
Water	Co-60 build-up cap[b]	0.4	1	0.9	1.3	3.4	···
	bare thimble[c]	negligible	2	0.2	0.2	1.3	shortest
Plastic	bare thimble	none	2 or more	0.3	0.3	2.3	···

[a]During transport of the chamber into the phantom medium.
[b]0.45-cm Lucite wall.
[c]The Co-60 build-up cap preexisted in thermal equilibrium with the water phantom at time zero, when the chamber was inserted into the phantom.

V. COMPARISON WITH EXPERIMENTAL DATA

Equations (3) and (7) were applied to (i) the 14.5-cm-thick plastic phantom cooling in air and (ii) the cylindrical ion chamber with build-up cap (0.46-cm Lucite wall) cooling in a water medium. We used thermal-parameter values[7] for generic plastic [$K = 0.000454$ cal/(s·cm·°C) and $C = 0.35$ cal/(g·°C)], and densities of 1.17 and 1.045 g/cm^3 for Lucite[8] and polystyrene (manufacturer's value), respectively. Values of plastic-phantom thickness, L, and cylinder radius, R, were selected through an interactive process to yield the same exponential fall-off as that of our experimental data. An effective phantom thickness of 17.8 cm and an effective cylinder radius of 0.7 cm were obtained.

In Fig. 7 the theoretical curves are compared with the measured data for the two experimental cases: (i) the plastic phantom cooling in air, and (ii) the Farmer-type chamber covered with the protective cap cooling in water. The theoretical curves reproduce the general features: the shoulder and the exponential fall-off. For the ion chamber with build-up cap, the theoretical curve for an ideal cylinder agrees well with the experimental data. For the plastic phantom, the broader than expected experimental shoulder width arises due to a significant departure from the theoretical geometry. The dominating departure probably stems from a lack of heat transfer through the phantom surface in contact with the insulating tabletop. However, Fig. 3 shows that the shoulder width is highly dependent on the position of the measurement point in the phantom, and Eq. (3) suggests that both slope and shoulder depend on thickness, L. Considering that the 30-cm-square experimental phantom is cooled through five surfaces, while the semi-infinite theoretical phantom is cooled through all surfaces, the level of agreement for a 17.8-cm-thick theoretical phantom and 14.5-cm-thick experimental phantom is considered acceptable.

VI. CONCLUSIONS

The results of thermal equilibration of an ion chamber when introduced into various phantom media are summarized in Table I. The table lists several important characteristics, namely, the shoulder width, the number of exponential components in the temperature fall-off region, and the half-life of the first exponential component.

The bare thimble equilibrates very rapidly in all media with virtually no shoulder. In air, the time interval for equilibration to 10% of the initial temperature difference is 3 min, while in water and in plastic phantoms, the intervals are just over 1 and 2 min, respectively.

Chambers in thermal equilibrium with their build-up (protective caps) equilibrate less rapidly and exhibit an initial shoulder, followed by an exponential fall-off. In water, equilibration to less than 10% of the initial temperature difference requires only a few minutes, whereas in air a quarter of an hour is required.

Plastic phantoms require a very long time to equilibrate, however, there is a significant shoulder of several hours. Therefore, if the temperature of the phantom cavity is measured, the shoulder may be exploited to assure no temperature change over a period of an hour or more.

ACKNOWLEDGMENTS

This work was supported by Public Health Service Grant No. CA10953 awarded by the National Cancer Institute, Department of Health and Human Services. We thank Dr. José BenComo for suggesting Ref. 6 and Professor N. L. Sharma, Department of Physics at Michigan State University, for providing advice on the theoretical analysis of the data. We also thank Elizabeth Shears for typing the many drafts of this manuscript.

[a)]For correspondence, address R. C. Tailor, Ph.D. at U.T. M.D. Anderson Cancer Center, 1515 Holcombe Blvd., Box 547, Houston, TX 77030; Phone: (713) 792-3226, Fax: (713) 794-1364, Electronic mail: Rtailor@mdanderson.org

[1]R. J. Barish, ''Thermal characteristics of a common polystyrene phantom,'' Med. Phys. **11**, 214–215 (1984).
[2]H. Kubo, ''Ionization chamber response to a sudden change of ambient temperature in air, water and a polystyrene phantom,'' Med. Phys. **10**, 676–679 (1983).
[3]P. H. van der Giessen, ''About the rate of temperature changes in a

thimble chamber,'' Radiot. Oncol. **7**, 287–291 (1986).
[4]C. S. Mayo and B. Gottschalk, ''Temperature coefficient of open thimble chambers,'' Phys. Med. Biol. **37**, 289–291 (1992).
[5]P. M. Morse and H. Feshbach, *Methods of Theoretical Physics*, Part II (McGraw-Hill, New York, 1953).
[6]H. S. Carslaw and J. C. Jaeger, *Conduction of Heat in Solids*, 2nd ed. (Clarendon, Oxford, 1986).
[7]*Handbook of Chemistry and Physics*, 58th ed. (CRC, Boca Raton, FL, 1977–78).
[8]American Association of Physicist in Medicine, RTG Task Group 21, ''A protocol for the determination of absorbed dose from high-energy photon and electron beams,'' Med. Phys. **10**, 741–771 (1983).